EMG-Based Gestures Classification Using a Mixed-Signal Neuromorphic Processing System

Yongqiang Ma, *Member, IEEE*, Badong Chen, *Senior Member, IEEE*, Pengju Ren, *Member, IEEE*, Nanning Zheng, *Fellow, IEEE*, Giacomo Indiveri, *Senior Member, IEEE*, and Elisa Donati, *Member, IEEE*

***Abstract*— The rapid increase of wearable sensor devices poses new challenges for implementing continuous real-time processing of physiological data. Neuromorphic sensory-processing devices can enable both the measurement of bio-signals and their processing locally in compact embedded wearable systems. In particular, mixed-signal spiking neural networks implemented on neuromorphic processors can be integrated directly with the sensors to extract temporal data-streams in real-time with very low power consumption. In this work, we present a neuromorphic approach for classifying spatio-temporal data from electromyography (EMG) signals, which paves the way toward the realization of compact wearable solutions for neuroprosthetic control. Here we extend previously proposed delta-encoding methods to transform bio-signals into spike trains and use a spiking Recurrent Neural Network (SRNN) architecture to extract features from them. The SRNN was first simulated in software to find the optimal set of hyperparameters, and then validated on the neuromorphic hardware, with a difference in the performance of less than 2%. We describe how biologically plausible mechanisms such as Spike-Timing Dependent Plasticity (STDP) and soft Winner-Take-All (WTA) networks can be exploited to classify the EMG signals and show how their combined use in EMG data classification achieves competitive results with different datasets. Specifically, the classification performance for the Roshambo EMG dataset, which has three different classes, is above 85%, and for the basic finger movements dataset from the Ninapro database, which has eight different classes, reaches 55% accuracy.**

***Index Terms*— Neuromorphic engineering, biomedical signal processing, spike encoding, spiking recurrent neural network , spike-based learning, Winner-Take-All.**

Manuscript received July 10, 2020; revised September 30, 2020; accepted November 2, 2020. Date of publication November 16, 2020; date of current version December 11, 2020. This work was supported in part by the National Science and Technology Major Project of China under Grant 2018ZX01028-101-001; in part by the National Natural Science Foundation of China under Grant 61773312, Grant 61773307, and Grant 91648208; in part by the EU-H2020 MSCA-IF Grant NEPSpiNN under Grant 753470; in part by the EU-H2020 FET Project CResPACE under Grant 732170; and in part by the EU-H2020 ERC project NeuroAgents under Grant 724295. This article was recommended by Guest Editor F. Conti. *(Corresponding author: Pengju Ren.)*

Yongqiang Ma, Badong Chen, Pengju Ren, and Nanning Zheng are with the Institute of Artificial Intelligence and Robotics, Xi'an Jiaotong University, Xi'an 710049, China (e-mail: musaqiang@stu.xjtu.edu.cn; chenbd@mail.xjtu.edu.cn; pengjuren@mail.xjtu.edu.cn; nnzheng@mail.xjtu.edu.cn).

Giacomo Indiveri and Elisa Donati are with the Institute of Neuroinformatics, University of Zurich, 8006 Zurich, Switzerland, and also with the ETH Zurich, 8092 Zurich, Switzerland (e-mail: giacomo@ini.uzh.ch; elisa@ini.uzh.ch).

Color versions of one or more figures in this article are available at https://doi.org/10.1109/JETCAS.2020.3037951.

Digital Object Identifier 10.1109/JETCAS.2020.3037951

I. Introduction

MODELING and exploration of Biological Neural Networks (BNNs) have attracted research from many different fields. In recent years progress in computational neuroscience has inspired the development of Artificial Neural Networks (ANNs) from BNNs. However, although the basic principles of learning and generalization of ANNs are derived from BNNs, their hardware implementation in Complementary Metal-Oxide Semiconductor (CMOS) technologies still cannot reach the performance of animal brains, with respect to the trade-off of power consumption, efficiency, and robustness.

Thanks to their functional similarity to the brain, Spiking Neural Networks (SNNs) bridge the properties of ANNs with those of BNNs. Compared to traditional ANNs, SNNs process information in pulses or "spikes", a more biologically plausible representation, which offer advantages in terms of energy efficiency and latency. Neuromorphic hardware platforms [1]–[6] are the ideal substrate for emulating SNNs and enable their deployment in real-world applications.

Since in these in-memory-computing platforms there is no access to long-term storage [7], spatio-temporal pattern classification tasks require a different approach to storing data. A widely used method is to use attractor networks and Recurrent Neural Networks (RNNs) [8], [9].

In this paper, we present a system that includes an adaptive method for encoding biomedical signals in spike trains, a SRNN for extracting features from the spike trains, and a learning network composed of STDP and WTA for performing classification. The SRNN was simulated using the neural network simulator NEST and validated directly on the neuromorphic device Dynamic Neuromorphic Asynchronous Processor (DYNAP) [6]. The effectiveness of entire system was verified on a surface EMG signals classification task.

Hardware implementations of SNNs on neuromorphic chips have been shown to be able to solve a broad range of problems [10]–[17]. Recently, they have also been applied to processing biomedical signals, such as EMG and electrocardiogram (ECG), to exploit their ability to process data with low latency and low power consumption [18]–[23].

Superficial EMG signals represent neuromuscular activation during voluntary contraction, and are measured by on-skin electrodes. In the rest of this paper we will use the acronym EMG to refer to superficial EMG. A key application of EMG

2156-3357 © 2020 IEEE. Personal use is permitted, but republication/redistribution requires IEEE permission.
See https://www.ieee.org/publications/rights/index.html for more information.

Authorized licensed use limited to: Bangladesh Univ of Engineering and Technology. Downloaded on April 14,2022 at 06:40:20 UTC from IEEE Xplore. Restrictions apply.

signal processing is the gesture discrimination, applied to neuroprosthetic control [24], [25].

In this work we used two different EMG datasets to verify the effectiveness of the system: i) collected by using a Myo armband during the execution of three different gestures (i.e. rock, paper, and scissors), ii) a Ninapro dataset, including eight different hand gestures, gathered using 12 active double-differential wireless electrodes from a Delsys Trigno Wireless EMG system. The EMG signals were then encoded into spike trains through a delta encoding converter algorithm [20], [26] with a new adaptive threshold selection method. The classification was implemented using a custom Python toolbox based on the NEST SNN simulator. A traditional machine learning method, such as the Support Vector Machine (SVM), was used as the baseline for a bio-inspired classification method that used STDP [27] learning rule and WTA computational principle [28].

While recurrent SNNs have already been used to classify EMG signals in previous work, here we employ them with the following new key contributions:

1) a novel adaptive delta-encoding method combined with the outliers removal and signal normalization processing, to keep the input firing rate equalized across channels and subjects
2) a sparse representation for the SRNN input data, reducing the number of connections in the SRNN
3) a soft WTA to combine with STDP learning to improve the network classification accuracy
4) comparison of the network performance with alternative frameworks, using different data sets.

Results show that the proposed SRNN architecture is a promising approach for EMG signal classification tasks.

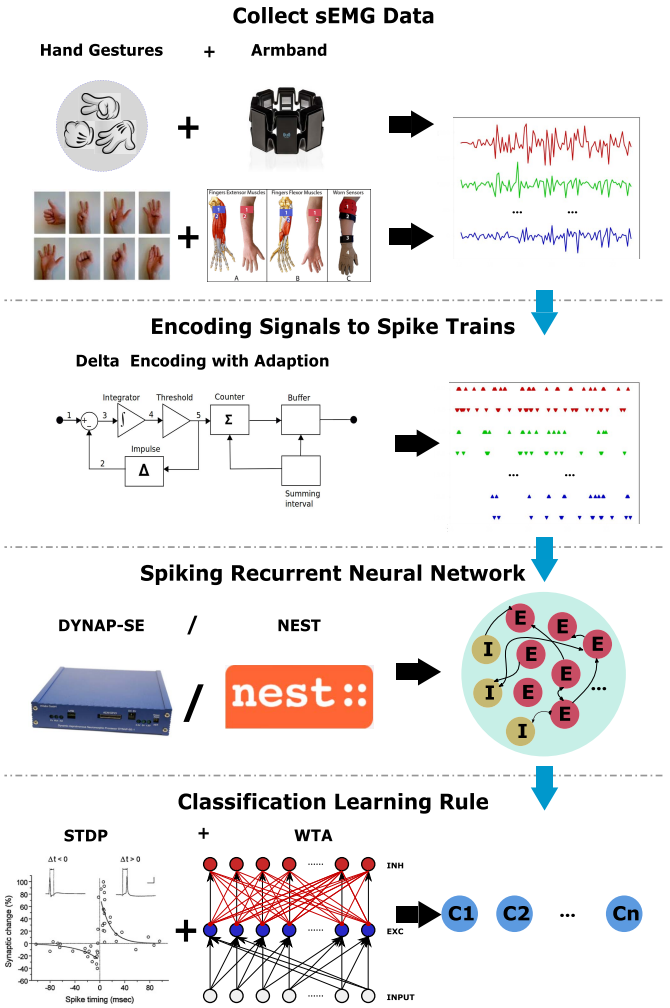

Fig. 1. Architecture of the gestures classification system. The system includes the data collecting phase, the spike encoding phase, the feature extraction phase by recurrent spiking neural network, and the classification learning phase. One of the EMG datasets is collected by using Myo armband and the other dataset is from Ninapro DB2. The signals are encoded into spike trains by a delta-converter algorithm with adaptation. The neuromorphic SRNN extracts the features that are then classified by using traditional machine learning and biologically plausible learning rules.

II. Materials and Methods

The overall architecture of the system is shown in Fig. 1. We propose a hardware-compatible SRNN architecture designed to classify gestures, validate with a hardware implementation on a neuromorphic chip.

We first prototyped the network using a software SNN simulator (NEST), we then mapped the parameters and architecture details onto the DYNAP chip, and stimulated it by sending spike-trains. The spike trains were encoded from EMG signals by using an adaptive encoding scheme based on a standard delta-encoding method [26]. The adaptation in the delta-converted, combined with the preprocessing techniques, such as the outliers removal and normalization, allows equalizing the mean firing rate of the input neurons encoding the analog EMG signals.

A. Electromyography Dataset

Two datasets were used to verify the effectiveness of the proposed approach. The first dataset was collected using the 8-channels Myo armband at 200 Hz. This dataset consists of 10 able-bodied subjects [29] recorded during the performance of 3 gestures: rock, paper, and scissor (i.e. Roshamboo dataset). Each gesture was recorded 5 times for 2 s per session, for a total of 3 sessions from each subject. Between every two gestures, there was a relaxing phase of 1 s where the muscles could go to the rest status, removing any residual muscular activation. In this paper, we investigated the steady-state by removing 600 ms from the start and end of each 2 s gesture. We then divided each 800 ms sample into four parts, each lasting 200 ms. The size of this window was chosen to respect the maximum classification latency affordable in prosthetic control [30]. The dataset included 1800 trials, 600 trials for each gesture, split in 1440 for training, and 360 for testing (4:1 ratio).

The second dataset is the Ninapro (Non Invasive Adaptive Prosthetics) DB2 [31] composed of 50 gestures from 40 able-bodied subjects sampled at a rate of 2 kHz. The measurement of muscle activity was gathered using 12 active double–differential wireless electrodes from a Delsys Trigno Wireless EMG system. The electrodes were positioned as follow: eight electrodes were equally spaced around the forearm in

Authorized licensed use limited to: Bangladesh Univ of Engineering and Technology. Downloaded on April 14,2022 at 06:40:20 UTC from IEEE Xplore. Restrictions apply.

correspondence to the radio humeral joint; two electrodes were placed on the main activity spots of the flexor digitorum and of the extensor digitorum; two electrodes were placed on the main activity spots of the biceps and of the triceps. Each hand gesture lasts 6 s and is repeated 6 times for every subject. There is a rest time between two gestures for the muscles to go back to the rest status and removing any residual muscular activation. In this paper, we selected 8 gestures of the basic movements of the fingers. As for the Roshamboo dataset the signals were cut in samples of 200 ms. In the selected dataset, there were 7680 trials divided into training (6144 records) and testing sets (1536 records) according to a 4:1 ratio. The Ninapro DB2 is widely used and in this paper, for the first time, was deployed to validate a neuromorphic network architecture.

To feed the EMG into the SNN, the signals need to be converted in spike trains. The delta-converter proposed in [26] represents a suitable conversion method for encoding continuous signals into spike trains. This encoding method presents special characteristics that enable low circuit complexity and low power consumption, and therefore make it a good solution for biomedical and wearable applications. The delta-encoding is also more flexible and reliable than multi-bit binary systems since it is independent of hardware structure and fault-tolerant to bit errors. For these reasons, is widely used in biomedical circuits and systems [32], [33].

In this paper, the delta-converter was integrated with an adaptive mechanism to keep the firing rate in a similar range across channels. This limits the channels with a high firing rate to influence and take over the entire network behavior.

B. Data Preprocessing and Encoding

The EMG signals are multi-channel continuous biological data records. As each channel is influenced by the external environment, physical difference of subjects, and electrodes displacement, the EMG data is very noisy. Therefore, to extract features from this data we preprocessed it before encoding using the following three steps:

1) Outliers Removal: During the data collection, external disturbances can cause outliers, as shown in Fig. 2A, highlighted in blue. These outliers significantly affect the encoding, which is sensitive to the changes in the input. We removed them by setting every value larger than the 99.98 percentile to 1 and those smaller than 0.02 percentile to 0. The rest of the data was converted according to Equation 1, where the Min_i equal to the 0.02 percentile and the Max_i equal to 99.98 percentile. After removing the outliers the distribution of EMG values became more balanced, as shown in the second column of Fig. 2. It also can increase the relative amplitude of the signal, as shown in Fig. 2 C and Fig. 2D.

2) Normalization: EMG signals from different subjects have different data distributions. Even for the same subject performing the same gesture, the EMG signals have large differences. To decrease these differences, the data were normalized between 0 and 1 using the following equation:

$$Data_i^{norm} = \frac{Data_i - Min_i}{Max_i - Min_i}, \tag{1}$$

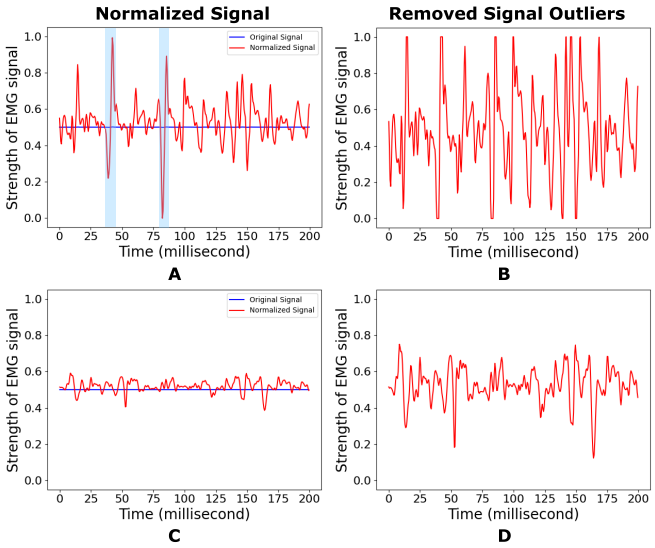

Fig. 2. The preprocessing of EMG signals: 1) Outliers removal. The outliers in panel A (highlighted in blue) are removed to obtain the signal in panel B. 2) Normalization across channels and gestures. The range of the signal in panel C increases after normalization as shown in panel D.

3) Data Segmentation and Selection: To perform experiments mimicking real-time scenarios, each signal was cut in chunks of 200 ms, as required in prosthetic applications [30]. In this work we investigated the signal at the steady-state and, therefore, the initial and final parts of the signal, that correspond to the gesture transitions, were ignored.

Afterwards, the EMG signals were encoded into spike trains using the adaptive delta-converter and fed into the SNN. To ensure similar spiking rates across gestures and channels we proposed an adaptation mechanism that can be expressed in pseudo-code as shown in the Algorithm 1.

Algorithm 1 Spike Encoding With Adaptation

```
Result: Encoded spike train.
Initialization: input signal, threshold; encode the input
signal into spike train with threshold by delta-encoding
method;
while spike rate > 120Hz or spike rate < 100Hz do
    if spike rate > 120Hz then
        threshold += 0.1;
    else
        threshold -= 0.1;
    end
    encode the input signal into spike train with threshold
    by delta-encoding method;
end
```

The key point of the adaptive mechanism is to find a suitable threshold for each sample of EMG signals to equalize the mean firing rates of the neurons. With fixed threshold settings equal for all samples, gestures that require low muscle activity would be encoded with low-frequency spike trains, while gestures that produce strong muscle responses would produce high firing rates, as shown in Fig. 3A and 3C.

Authorized licensed use limited to: Bangladesh Univ of Engineering and Technology. Downloaded on April 14,2022 at 06:40:20 UTC from IEEE Xplore. Restrictions apply.

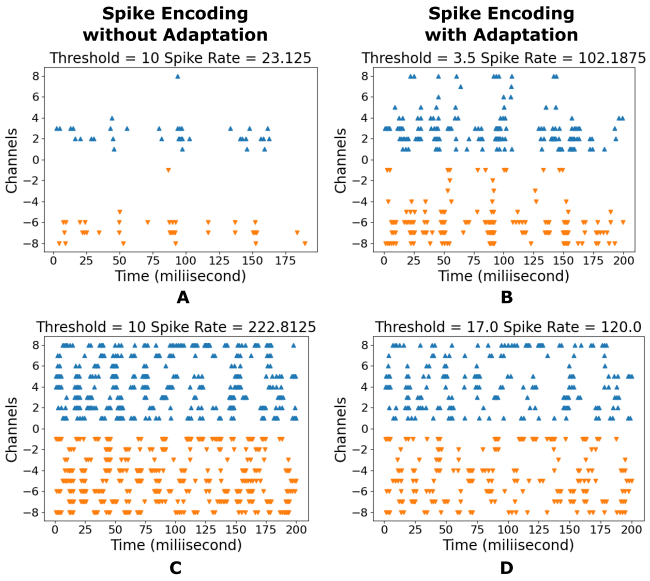

Fig. 3. Spike encoding from preprocessed EMG signals. Without adaptation, when the threshold is fixed for the delta-encoding method, weak signals are encoded into low-frequency spike trains as shown in (A); on the contrary, strong signals will be encoded with high-frequency spike trains as shown in (C). However, the adaptation method finds a threshold for encoding signals with a suitable firing rate range (see (B) and (D)).

In our encoding algorithm, we used a loop to adjust the magnitude of the threshold to find the suitable value for equalizing the spiking rates, while limiting the threshold in a suitable range. Here we kept the threshold value between 1 and 50 to make the rate of spike trains between 100 Hz and 120 Hz after encoding, such as Fig. 3B and 3D shown.

The adaptive delta-converter algorithm, produces an UP and DOWN spike train for each channel, according to the positive or negative changes in the signal. For each EMG channel, two spike trains are produced that are connected to neurons inside the SRNN with excitatory synapses.

C. Neuromorphic Hardware

The proposed SRNN was simulated in the NEST framework, and as well as implemented on the DYNAP chip. The DYNAP is a fully customized mixed-signal neuromorphic chip with massively parallel analog spiking neuron circuits and asynchronous digital event-based routing circuits which allow the implementation of reconfigurable and real-time SNNs [6]. The current-mode sub-threshold synapse circuits [34] in the chip directly emulate the dynamics of biological synapses in real-time, and realize the temporal integration of input spikes. As the biologically plausible time constants of the synapse and neuron circuits can be set to be compatible with the temporal scale of the EMG signals, the system can be configured to implement matched filters for optimal signal processing and classification with very low power [7], [35].

Each DYNAP board contains 4 chips where each chip comprises 4 cores of 256 adaptive exponential integrate-and-fire neurons (AEI&F), for a total of 4096 neurons for one board. Four different kinds of synapses can be chosen: slow excitatory, fast excitatory, slow inhibitory, and fast inhibitory synapse. Each neuron has a Content Addressable Memory (CAM) block that contains 64 addresses, which can be programmed to match the Address-Events representing the identity of any other neuron in the chip. The Address-Event Representation (AER) communication protocol [36] is used to receive and transmit spikes between digital peripheral asynchronous input/output logic circuits with the chip. It allows flexible connectivity with microsecond precision under heavy system loads by a fully asynchronous inter-core and inter-chip routing architecture. Each core of the DYNAP chip has programmable bias generator circuits that can be configured to control the behavior and dynamics of the neurons and synapses.

TABLE I

TYPE AND CONNECTION PROPORTION OF SYNAPSES BETWEEN GROUPS OF NEURONS ON DYNAP

pre-synapse	post-synapse	
	excitatory	inhibitory
input	FAST_EXC : 3.125%	-
excitatory	SLOW_EXC : 2.5%	SLOW_EXC : 3.75%
inhibitory	SLOW_INH : 3.75%	-

D. Spiking Recurrent Neural Network

The SNN on both NEST simulator and the DYNAP chip is a RNN and was used as a feature extractor capable of separating spike trains features by increasing their spatial dimensionality.

The proposed SRNN is composed of 256 excitatory neurons and 64 inhibitory neurons. On the DYNAP, these two sets of neurons were assigned to two different cores of the same chip: the excitatory neurons were organized as a 16×16 array on one core, and the inhibitory neurons as an 8×8 array on another core. Neurons in the same core shared the same parameters. Each spike train was sent to 8 randomly selected excitatory neurons, each of which only received one input spike train. The excitatory neurons were randomly connected, whereas there was no connection among inhibitory neurons. The connections between the excitatory and inhibitory neurons were bidirectional. All the connections between different neuron groups were randomly chosen by a low proportion (see Table I). Indeed, if the connections are too dense or strong, each neuron will affect its afferents and synchronization effects will degrade performance. Table I shows the type of synapses between different kinds of neuron groups and the connectivity ratios on-chip.

The inhibitory neurons ensure network stability. They are activated by excitatory neurons and their activity is sufficient to decrease the network activation. We tuned the biases of the neurons to obtain different SRNN output for different gestures and reduce the effect of network noise for the same gesture. In particular, the important parameters are the neuron threshold V_{thr}, the decay time constant of the membrane τ_m, and the decay time constant of the synapse τ_s. The details of the parameters set for the simulator and the chip are shown in Section III.

Authorized licensed use limited to: Bangladesh Univ of Engineering and Technology. Downloaded on April 14,2022 at 06:40:20 UTC from IEEE Xplore. Restrictions apply.

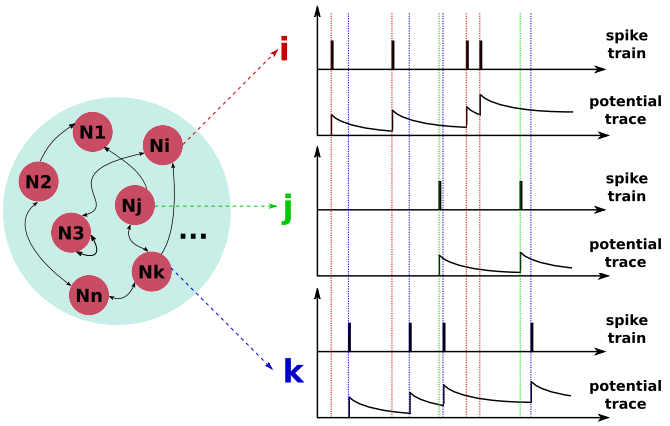

Fig. 4. The neuron potential trace of excitatory neurons in SRNN. The trace records the spikes and membrane potential of the neuron on the timeline which can be used to update the synaptic weight between SRNN and WTA excitatory neurons by STDP.

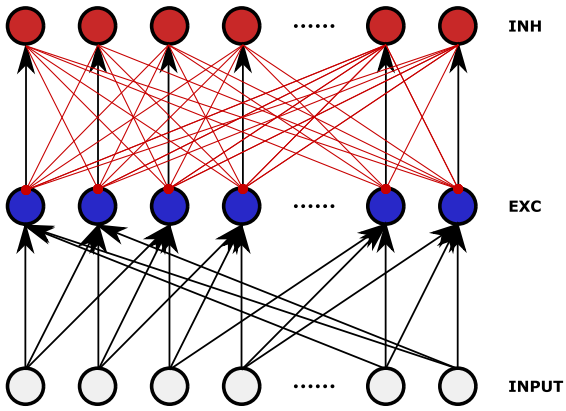

Fig. 5. Structure of the WTA network. Input neurons are randomly connected to excitatory neurons. Excitatory neurons are connected to inhibitory neurons with a one-to-one strategy, and each inhibitory neuron connects to all the excitatory neurons except the pre-synaptic one.

E. Classification With STDP and WTA

To classify the hand gestures, the network output was trained using a learning rule which combines STDP and WTA. The STDP learning part included 256 excitatory neurons and an equal number of inhibitory neurons. The output spike trains of the excitatory neurons of the SRNN were fed into the excitatory neurons of the learning part. In particular, the excitatory neurons of the SRNN and the excitatory neurons of WTA were all-to-all connected with random weights trained by the STDP based learning rule. The weight update rule is the following:

$$\Delta w = \begin{cases} -a_{pre} \cdot e^{-\frac{t_{post}-t_{pre}}{\tau_{syn}}} & \text{for pre-synapse} \\ a_{post} \cdot e^{-\frac{t_{post}-t_{pre}}{\tau_{syn}}} & \text{for post-synapse,} \end{cases} \tag{2}$$

where a_{pre} and a_{post} represent the learning rates for the spike firing in pre- and post-synapse neuron respectively, t_{pre} and t_{post} correspond to the timing of the pre-synaptic and post-synaptic spikes respectively. The τ_{syn} is the time constant that determines the learning time window. After the update, the synaptic weights should be normalized as follows:

$$w_{ij}^{norm} = \frac{w_{ij}}{\sum_i w_{ij}} \cdot w_{sum}^{tar} \tag{3}$$

where w_{ij} is the synaptic weight from the i^{th} excitatory neuron of SRNN to the j^{th} excitatory neuron of WTA network, and w_{sum}^{tar} is the sum of postsynaptic weights from an excitatory neuron in the WTA network after normalization.

In the software simulations, the synaptic trace was used to compute the weight update dynamics, improving the learning speed [37]. For each synapse, we kept track of the trace of the presynaptic spike history and updated the weight accordingly to the following rule: the presynaptic trace tr_{pre} is increased by 1 when a presynaptic spike arrives at the synapse ($t = t_{spike}$) and then decays exponentially. The decay is described by the following equation:

$$tr_{pre} = \begin{cases} tr_{pre} + 1 & t = t_{spike} \\ tr_{pre} \cdot e^{-\frac{t_{cur}-t_{fir}}{\tau_{tr}}} & \text{other times} \end{cases} \tag{4}$$

where t_{cur} is the current time and t_{fir} is the last firing time of presynaptic spike, τ_{tr} is the time constant of synapse which can control the decay speed of presynaptic trace. The larger the τ_{tr} is, the faster the presynaptic trace will decay. Figure 4 shows the potential trace changes of some excitatory neurons in SRNN. Once the presynaptic spike arrives at the synapse, the synaptic weight will be updated based on the presynaptic trace following Equation 5:

$$\Delta w = \begin{cases} a_{pre} \cdot (tr_{pre} - tr_{tar}) & \text{for pre-synapse} \\ a_{post} \cdot (tr_{pre} - tr_{tar}) & \text{for post-synapse} \end{cases} \tag{5}$$

where tr_{tar} is the expected target value of presynaptic trace at the moment of a postsynaptic spike. From Equation 5, it is evident that the expected target value of presynaptic trace is inversely proportional to the synaptic weight. The STDP synapses are normalized whenever they update N times by N samples of EMG signals. This allows us keeping the sum of the postsynaptic weights from an excitatory neuron in WTA network within bounds.

The excitatory neurons are one-to-one connected to the inhibitory neurons in the learning layer, and each spike in the excitatory pool triggers the activation of the corresponding inhibitory neuron. Each inhibitory neuron connects to all excitatory neurons, except for the pre-synaptic one. This connection strategy causes competition between excitatory neurons through the lateral inhibition, achieving the WTA structure, as shown in Fig. 5. The classical WTA network chooses as the winner the neuron with the highest firing rate. Nevertheless, the network is sensitive to parameters change, thus if the weight between inhibitory and excitatory synapses is too weak, the lateral inhibition cannot influence the activity of the neurons. On the other hand, strong inhibition prevents other neurons to fire once a winner has been chosen. The EMG signals are noisy and subject-dependent, therefore the winner selected by the classical WTA is not sufficient to include all the signal information. To increase the robustness of the learning rule, we used a soft WTA which allows several winners and only inhibits the weakest neurons.

Since the soft WTA allows multiple winner neurons, and the number of winners is not fixed, it is difficult to com-

Authorized licensed use limited to: Bangladesh Univ of Engineering and Technology. Downloaded on April 14,2022 at 06:40:20 UTC from IEEE Xplore. Restrictions apply.

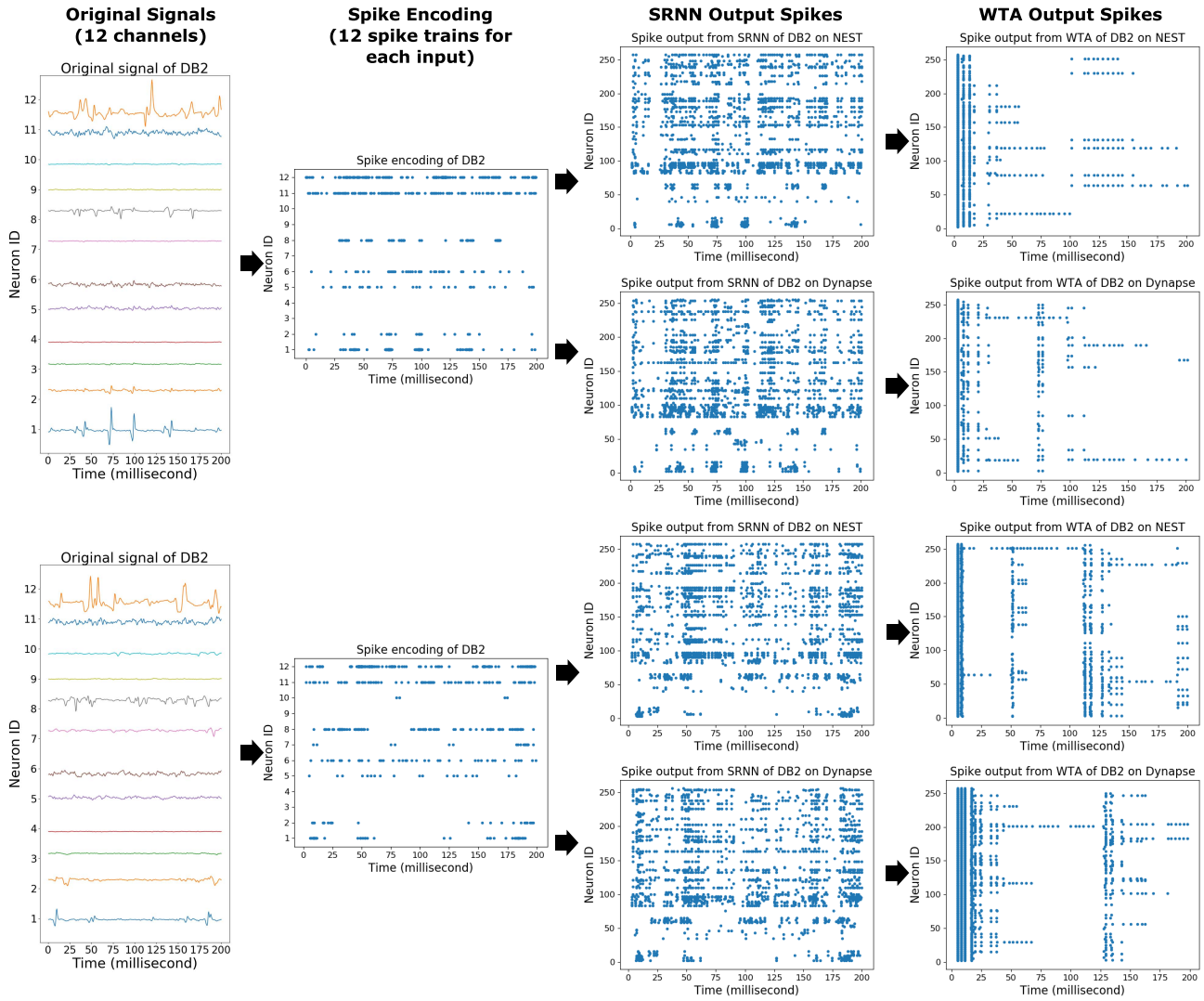

Fig. 6. System steps for two different gestures on both DYNAP and NEST. The original signal of EMG, which has 12 channels, are encoded into 24 spike trains by delta-converter with adaptation, and then fed into the SRNN.

pare two samples. To solve this drawback we proposed an approach inspired by networks developed to model how similar visual inputs produce similar dynamic state activities in monkeys [38]. The spiking rate of the excitatory neurons of the soft WTA network can be used as a vector to represent the network's dynamic state. The classification was done by comparing the distance between these vectors: different gestures produce larger differences than the ones produced by similar gestures. The classification was performed by comparing the distance between the vectors. In particular, we computed the Euclidean distance, following Algorithm 2, to show that the inter-classes distance is larger than the intra-classes one, thereby allowing to classify the input gestures as different clusters.

III. Analysis and Results

To verify the classification performance, two datasets (Roshambo dataset and Ninapro DB2 dataset) were used, as described in Section II-A. First, the SRNN was simulated in NEST to test the effectiveness of the network in a noise-free environment. Then the neuromorphic chip DYNAP was used to test the robustness of the SRNN in an analog circuit environment. Both software-based and hardware-based platforms used the same network structure. Given the limitations of the DYNAP chip, only 256 excitatory neurons were used in the SRNN. In Fig. 6, we show the output of every system step, from the original signal to the WTA for the Ninapro DB2 dataset.

A. Experimental Parameter Settings and Results

The proposed system is based on spiking neurons, in Table II we list all pre- and post-synapse of neurons and the ratio of connections between different groups. The connections among SRNN were very sparse to keep the network able to respond differently to different features. In the STDP learning rule, the learning rates were set as $a_{pre} = 0.9 \cdot a_{post} = 1 \times 10^{-6}$ for Roshambo dataset and $a_{pre} = 0.9 \cdot a_{post} = 5 \times 10^{-7}$ for Ninapro DB2 dataset, where a_{pre} and a_{post} are the learning rates for the spike firing in pre- and post-synapse respectively, and the synapse time constant is $\tau_{syn} = 10\,ms$. The changes in the synaptic weights only happened once a spike was triggered.

Authorized licensed use limited to: Bangladesh Univ of Engineering and Technology. Downloaded on April 14,2022 at 06:40:20 UTC from IEEE Xplore. Restrictions apply.

Algorithm 2 Classification by Comparing the Euclidean Distance

Result: Test label ts_label.
Initialization: training dataset tr_set, test data ts_data;
make the tr_set as a standard library std_lib for the test dataset;
while *std_lib is not empty* **do**
  min_distance = Inf;
  calculate the Euclidean distance euc_dist between ts_data and tr_data from std_lib;
  if *min_distance > euc_dist* **then**
    min_distance = euc_dist;
    set test label equal to training data label ts_label = tr_label;
  end
end

TABLE II
THE CONNECTION BETWEEN DIFFERENT NEURON GROUPS IN THE SYSTEM

			post-synapse			
			SRNN		WTA	
			EXC	INH	EXC	INH
pre-synapse	input	EXC	3.125%	—	—	—
	SRNN	EXC	2.5%	3.75%	all to all	—
		INH	3.75%	—	—	—
	WTA	EXC	—	—	—	one to one
		INH	—	—	one to all[1]	—

We performed the EMG classification by using STDP learning rule with WTA bio-inspired strategy. The spiking rate of neurons during the training phase was saved to provide a labeled activity. During testing, the distance between the spiking rate of the neurons and the labeled activity was used to classify the samples.

For the Roshambo dataset, the classification accuracy of the NEST simulation was 85.28%, while the DYNAP one was 83.61%. When using SVM to classify the extracted features (output spike trains from SRNN of excitatory neurons), the accuracy of classification was 75% with NEST and 76% with DYNAP. For the Ninapro DB2 dataset, the accuracy was 57.23% with the NEST simulations and 55.92% with the DYNAP chip. Using SVM the classification accuracy was 36% with NEST and 35% with DYNAP. From these results, we can see that there is no significant difference between the SRNN on the simulator and the analog chip.

Figure 7 shows the confusion matrix of EMG classification measured across different datasets and different platforms. Some hand gestures are harder to discriminate as they involve similar muscle activations (e.g. scissors and paper from the Roshambo dataset, and hand gesture 4 and 5 of the Ninapro DB2 dataset). However, the number of true positives is significantly larger than the others for each class.

[1]one to all connection without the one as pre-synapse neuron

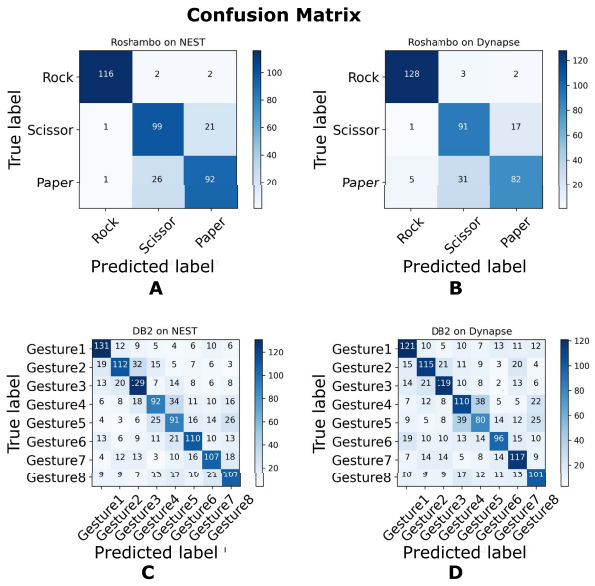

Fig. 7. Confusion matrix of EMG signals classification. In (A) and (B) show that the hand gestures scissor and paper are easier to confuse, this phenomenon also happens in the Ninapro DB2 dataset, such as (C) and (D), because some hand gestures require similar muscle movement in the forearm. For each hand gesture, the correct classification results are significantly higher than others.

B. Power Consumption

The power consumption of a silicon neuron n on the DYNAP can be estimated as follows, as proposed in [17]:

$$P_n = r_{in} \cdot (E_{sp} + E_{pl}) + r_{ou} \cdot (E_{en} + E_{br} + RT \cdot E_{rt}) \quad (6)$$

where r_{in} and r_{ou} represent mean input and output spiking firing rate respectively; from [6] we know that $E_{sp} = 883\ pJ$ is the energy used by the DYNAP neuron circuits to generate one spike; $E_{pl} = 324\ pJ$ is the energy of the pulse extender circuit; $E_{en} = 883\ pJ$ is energy to encode one spike and append the destination address; $E_{br} = 6.84\ nJ$ is the energy required to broadcast the event to a whole core; $E_{rt} = 360\ pJ$ is energy required to route an event to a different core; $RT = 1$ if the spike is sent to a different core, and zero otherwise.

Based on Equation 6, we estimated the power consumption of the proposed SRNN during the EMG classification task. The results are presented in Table III. For the Roshambo dataset, the average power consumption was 1.121 μW, and it was 1.19 μW for the Ninapro DB2 dataset. The inhibitory neuron group consumes more power because, to keep the SRNN in a stable state, it must fire at a higher rate compared to the excitatory group.

IV. DISCUSSION AND CONCLUSIONS

In this paper we proposed an SRNN system for on-line EMG classification, extending our work recently proposed in [39], to improve accuracy and classification performance on the Roshambo dataset. An important novel aspect of the new system is the introduction of an adaptive mechanism in the spike encoding front-end, which equalizes the spike rates

Authorized licensed use limited to: Bangladesh Univ of Engineering and Technology. Downloaded on April 14,2022 at 06:40:20 UTC from IEEE Xplore. Restrictions apply.

TABLE III
POWER CONSUMPTION ESTIMATE FOR CLASSIFYING SIGNALS FROM DIFFERENT DATASETS USING A DYNAP IMPLEMENTATION OF THE SRNN

Dataset	Excitatory Neurons	Inhibitory Neurons	All Neurons
Roshambo	$0.276\ \mu W$	$0.845\ \mu W$	$1.121\ \mu W$
NinaPro DB2	$0.344\ \mu W$	$0.846\ \mu W$	$1.190\ \mu W$

used to encode the continuous EMG signals while preserving the SRNN network's ability to extract effective features. A second novel contribution is the introduction of a STDP learning rule combined with a WTA network post-processing module which also contributes to increased performance in the classification task. The introduction of the WTA module was crucial, as previous attempts to use STDP learning alone could not converge effectively [39].

The proposed system is competitive, compared to other neuromorphic approaches presented in the literature. In [20], the authors set up a single layer SNN on the DYNAP chip and obtain 74% accuracy on the Roshambo dataset, while our system can reach accuracy levels of almost 85%. In [23], the authors compared the performances of three digital systems, Loihi [4] and ODIN+MorphIC [5], [40] when performing sensor fusion of EMG signals and event-based images to classify five hand gestures from sign language. The individual EMG was classified by using a spiking Multi-Layer Perceptron (MLP), reaching 55.7% and 53.6% of accuracy respectively. Our system reaches about 55% for eight categories of EMG signals classification. Although the accuracy of our system on the Ninapro DB2 dataset is inferior to the one obtained with conventional machine learning methods (e.g. that can reach about 78% accuracy with Convolutional Neural Network (CNN) software simulations [41]), the overall real-time performance can still provide some advantages if low-latency and low power-consumption features are important requirements. A thorough comparative analysis of the system proposed with more conventional ANN or DSP signal processing based methods would require a full end-to-end system performance comparison. While this is an important goal that we and the whole neuromorphic community have set, it is not something that could be achieved within this study.

The EMG data was encoded into spike trains by using a delta-encoding algorithm, and the resulting spike trains were then fed into the SRNN to extract both the spatial and temporal features representing a gesture movement. We used the SVM as a benchmark to assess the performance of the biological learning methods proposed. The spike-rate central distance classification method shows better performance than the SVM benchmark. For each input, the rate-based classification method produces about 1000 output spikes. Since on the DYNAP chip each neuron consumes 17 pJ at 1.3 V_{dd} power supply [6] to produce a spike, the mixed analog/digital neuromorphic core can achieve gesture classification with sub-mW power consumption figures (see Table III). As the accuracy of trace-based STDP learning is not very high, the system proposed is suitable for applications that can tolerate some errors, but that requires ultra-low-power and real-time performance. Future work will focus on implementing and further optimizing on-chip learning based on the results of this work. The hardware implementation of the SRNN presented here can classify gestures using biologically inspired learning rules. By including neuromorphic circuits for bio-signal sensing and spike-train encoding, such as those recently proposed in [42], it will be possible to develop compact embedded and ultra-low-power electronic systems able to classify EMG temporal data in real-time.

ACKNOWLEDGMENT

The authors would like to thank the China Scholarship Council (CSC) for the support. The authors also would like to thank the INI members Jingyue Zhao and Vanessa Leite who provide their neuromorphic chips DYNAP to run SRNN, Dmitrii Zendrikov who guided the bias tuning procedures to find the best parameters on the DYNAP, and Nicoletta Risi for help in estimating the DYNAP power consumption.

REFERENCES

[1] J. Schemmel, D. Briiderle, A. Griibl, M. Hock, K. Meier, and S. Millner, "A wafer-scale neuromorphic hardware system for large-scale neural modeling," in *Proc. IEEE Int. Symp. Circuits Syst.*, May 2010, pp. 1947–1950.

[2] S. B. Furber, F. Galluppi, S. Temple, and L. A. Plana, "The Spinnaker project," *Proc. IEEE*, vol. 102, no. 5, pp. 652–665, May 2014.

[3] P. A. Merolla *et al.*, "A million spiking-neuron integrated circuit with a scalable communication network and interface," *Science*, vol. 345, no. 6197, pp. 668–673, Aug. 2014.

[4] M. Davies *et al.*, "Loihi: A neuromorphic manycore processor with on-chip learning," *IEEE Micro*, vol. 38, no. 1, pp. 82–99, Jan. 2018.

[5] J. D. Legat, and D. Bol, "MorphIC: A 65-nm 738k-synapse/mm^2 quad-core binary-weight digital neuromorphic processor with stochastic spike-driven online learning," *IEEE Trans. Biomed. Circuits Syst.*, vol. 13, no. 5, pp. 999–1010, Dec. 2019.

[6] N. Qiao, F. Stefanini, and G. Indiveri, "A scalable multicore architecture with heterogeneous memory structures for dynamic neuromorphic asynchronous processors DYNAPS," *IEEE Trans. Biomed. Circuits Syst.*, vol. 12, no. 1, pp. 106–122, Oct. 2017.

[7] Y. Sandamirskaya, "The importance of space and time for signal processing in neuromorphic agents," *IEEE Signal Process. Mag.*, vol. 36, no. 6, pp. 16–28, Dec. 2019.

[8] W. Maass, T. Natschläger, and H. Markram, "Real-time computing without stable states: A new framework for neural computation based on perturbations," *Neural Comput.*, vol. 14, no. 11, pp. 2531–2560, Nov. 2002.

[9] H. Jaeger, "The echo state approach to analysing and training recurrent neural networks-with an erratum note," German Nat. Res. Center Inf. Technol., Bonn, Germany, Tech. Rep. 148, 2013.

[10] M. B. Milde *et al.*, "Obstacle avoidance and target acquisition for robot navigation using a mixed signal analog/digital neuromorphic processing system," *Frontiers Neurorobotics*, vol. 11, p. 28, Jul. 2017.

[11] J. Friedrich and M. Lengyel, "Goal-directed decision making with spiking neurons," *J. Neurosci.*, vol. 36, no. 5, pp. 1529–1546, Feb. 2016.

[12] J. Martel, R. Kreiser, N. Qiao, and Y. Sandamirskaya, "Adaptive motor control and learning in a spiking neural network realised on a mixed-signal neuromorphic processor," in *Proc. Int. Conf. Robot. Automat. (ICRA)*, May 2019, pp. 9631–9637.

[13] E. Donati, F. Perez-Pena, C. Bartolozzi, G. Indiveri, and E. Chicca, "Open-loop neuromorphic controller implemented on VLSI devices," in *Proc. 7th IEEE Int. Conf. Biomed. Robot. Biomechatronics (Biorob)*, Aug. 2018, pp. 827–832.

[14] J. Zhao, E. Donati, and G. Indiveri, "Neuromorphic implementation of spiking relational neural network for motor control," in *Proc. 2nd IEEE Int. Conf. Artif. Intell. Circuits Syst. (AICAS)*, Aug. 2020, pp. 89–93.

[15] J. Zhao, N. Risi, M. Monforte, C. Bartolozzi, G. Indiveri, and E. Donati, "Closed-loop spiking control on a neuromorphic processor implemented on the iCub," 2020, *arXiv:2009.09081*. [Online]. Available: http://arxiv.org/abs/2009.09081

Authorized licensed use limited to: Bangladesh Univ of Engineering and Technology. Downloaded on April 14,2022 at 06:40:20 UTC from IEEE Xplore. Restrictions apply.

[16] J. Rouat, D. Pressnitzer, and S. Thorpe, "Exploration of rank order coding with spiking neural networks for speech recognition," in *Proc. IEEE Int. Joint Conf. Neural Netw.*, vol. 4, Jul. 2005, pp. 2076–2080.
[17] N. Risi, A. Aimar, E. Donati, S. Solinas, and G. Indiveri, "A spike-based neuromorphic architecture of stereo vision," *Frontiers Neurorobotics*, vol. 14, p. 93, May 2020.
[18] J. Behrenbeck, Z. Tayeb, C. Bhiri, C. Richter, O. Rhodes, N. Kasabov, J. Conradt, "Classification and regression of spatio-temporal signals using NeuCube and its realization on Spinnaker neuromorphic hardware," *J. Neural Eng.*, vol. 16, no. 2, 2018, Art. no. 026014.
[19] E. Donati *et al.*, "Processing EMG signals using reservoir computing on an event-based neuromorphic system," in *Proc. IEEE Biomed. Circuits Syst. Conf. (BioCAS)*, Oct. 2018, pp. 1–4.
[20] E. Donati, M. Payvand, N. Risi, R. Krause, and G. Indiveri, "Discrimination of EMG signals using a neuromorphic implementation of a spiking neural network," *IEEE Trans. Biomed. Circuits Syst.*, vol. 13, no. 5, pp. 795–803, Oct. 2019.
[21] F. C. Bauer, D. R. Muir, and G. Indiveri, "Real-time ultra-low power ECG anomaly detection using an event-driven neuromorphic processor," *IEEE Trans. Biomed. Circuits Syst.*, vol. 13, no. 6, pp. 1575–1582, Dec. 2019.
[22] F. Corradi *et al.*, "ECG-based heartbeat classification in neuromorphic hardware," in *Proc. Int. Joint Conf. Neural Netw. (IJCNN)*, Jul. 2019, pp. 1–8.
[23] E. Ceolini *et al.*, "Hand-gesture recognition based on EMG and event-based camera sensor fusion: A benchmark in neuromorphic computing," *Frontiers Neurosci.*, vol. 14, p. 637, Aug. 2020.
[24] D. Farina *et al.*, "The extraction of neural information from the surface EMG for the control of upper-limb prostheses: Emerging avenues and challenges," *IEEE Trans. Neural Syst. Rehabil. Eng.*, vol. 22, no. 4, pp. 797–809, Jul. 2014.
[25] I. Batzianoulis, S. El-Khoury, E. Pirondini, M. Coscia, S. Micera, and A. Billard, "EMG-based decoding of grasp gestures in reaching-to-grasping motions," *Robot. Auto. Syst.*, vol. 91, pp. 59–70, May 2017.
[26] F. Corradi and G. Indiveri, "A neuromorphic event-based neural recording system for smart brain-machine-interfaces," *IEEE Trans. Biomed. Circuits Syst.*, vol. 9, no. 5, pp. 699–709, Oct. 2015.
[27] Y. Dan and M.-M. Poo, "Spike timing-dependent plasticity of neural circuits," *Neuron*, vol. 44, no. 1, pp. 23–30, Sep. 2004.
[28] P. U. Diehl and M. Cook, "Unsupervised learning of digit recognition using spike-timing-dependent plasticity," *Frontiers Comput. Neurosci.*, vol. 9, Aug. 2015.
[29] E. Donati, "EMG from forearm datasets for hand gestures recognition," Zenodo, Inst. Neuroinform., UZH/ETH, Zürich, Switzerland, Tech. Rep., 2019. [Online]. Available: https://zenodo.org/record/3194792, doi: 10.5281/zenodo.3194792.
[30] L. H. Smith, L. J. Hargrove, B. A. Lock, and T. A. Kuiken, "Determining the optimal window length for pattern recognition-based myoelectric control: Balancing the competing effects of classification error and controller delay," *IEEE Trans. Neural Syst. Rehabil. Eng.*, vol. 19, no. 2, pp. 186–192, Apr. 2011.
[31] M. Atzori *et al.*, "Electromyography data for non-invasive naturally-controlled robotic hand prostheses," *Sci. Data*, vol. 1, no. 1, pp. 1–13, Dec. 2014.
[32] C. Qian, J. Shi, J. Parramon, and E. Sanchez-Sinencio, "A low-power configurable neural recording system for epileptic seizure detection," *IEEE Trans. Biomed. Circuits Syst.*, vol. 7, no. 4, pp. 499–512, Aug. 2013.
[33] J. R. Custodio, J. Goes, N. Paulino, Oliveira, and E. Bruun, "A 1.2-V 165-/spl mu/W 0.29-mm2 multibit sigma-delta ADC for hearing aids using nonlinear DACs and with over 91 dB dynamic-range," *IEEE Trans. Biomed. Circuits Syst.*, vol. 7, no. 3, pp. 376–385, Jun. 2013.
[34] C. Bartolozzi and G. Indiveri, "Synaptic dynamics in analog VLSI," *Neural Comput.*, vol. 19, no. 10, pp. 2581–2603, Oct. 2007.
[35] E. Chicca, F. Stefanini, C. Bartolozzi, and G. Indiveri, "Neuromorphic electronic circuits for building autonomous cognitive systems," *Proc. IEEE*, vol. 102, no. 9, pp. 1367–1388, Sep. 2014.
[36] S. R. Deiss, R. J. Douglas, and A. M. Whatley, "A pulse-coded communications infrastructure for neuromorphic systems," in *Proc. Pulsed Neural Netw.*, Dec. 1999, pp. 157–178.
[37] A. Morrison, A. Aertsen, and M. Diesmann, "Spike-timing-dependent plasticity in balanced random networks," *Neural Comput.*, vol. 19, no. 6, pp. 1437–1467, Jun. 2007.
[38] D. L. K. Yamins, H. Hong, C. F. Cadieu, E. A. Solomon, D. Seibert, and J. J. DiCarlo, "Performance-optimized hierarchical models predict neural responses in higher visual cortex," *Proc. Nat. Acad. Sci. USA*, vol. 111, no. 23, pp. 8619–8624, Jun. 2014.
[39] Y. Ma, E. Donati, B. Chen, P. Ren, N. Zheng, and G. Indiveri, "Neuromorphic implementation of a recurrent neural network for EMG classification," in *Proc. 2nd IEEE Int. Conf. Artif. Intell. Circuits Syst. (AICAS)*, Aug. 2020, pp. 69–73.
[40] C. Frenkel, M. Lefebvre, J. D. Legat, and D. Bol, "A 0.086-mm ^{2}12.7-pj/sop 64k-synapse 256-neuron online-learning digital spiking neuromorphic processor in 28-nm CMOS," *IEEE Trans. Biomed. Circuits Syst.*, vol. 13, no. 1, pp. 145–158, Dec. 2018.
[41] X. Zhai, B. Jelfs, R. H. M. Chan, and C. Tin, "Self-recalibrating surface EMG pattern recognition for neuroprosthesis control based on convolutional neural network," *Frontiers Neurosci.*, vol. 11, p. 379, Jul. 2017.
[42] M. Sharifshazileh, K. Burelo, T. Fedele, J. Sarnthein, and G. Indiveri, "A neuromorphic device for detecting high-frequency oscillations in human iEEG," in *Proc. 26th IEEE Int. Conf. Electron., Circuits Syst. (ICECS)*, Nov. 2019, pp. 69–72.

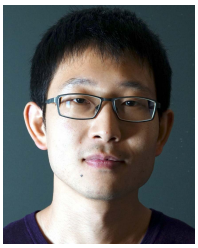

Yongqiang Ma (Member, IEEE) received the master's degree in software engineering from Xi'an Jiaotong University, Xi'an, China, in 2015, where he is currently pursuing the Ph.D. degree with the Institute of Artificial Intelligence and Robotics.

His current research interests include neuromorphic computing, neural network, and cognitive computing.

Badong Chen (Senior Member, IEEE) received the B.S. and M.S. degrees in control theory and engineering from Chongqing University, Chongqing, China, in 1997 and 2003, respectively, and the Ph.D. degree in computer science and technology from Tsinghua University, Beijing, China, in 2008.

He was a Post-Doctoral Researcher with Tsinghua University from 2008 to 2010, and a Post-Doctoral Associate with the Computational NeuroEngineering Laboratory, University of Florida, Gainesville, FL, USA, from 2010 to 2012. He visited the Nanyang Technological University, Singapore, as a Visiting Research Scientist for one month in 2015. He is currently a Professor with the Institute of Artificial Intelligence and Robotics, Xi'an Jiaotong University, Xi'an, China. He has published two books, four chapters, and over 200 papers in various journals and conference proceedings. His current research interests include signal processing, information theory, machine learning, and their applications to cognitive science and neural engineering.

Dr. Chen is a Technical Committee Member of the IEEE SPS Machine Learning for Signal Processing and the IEEE CIS Cognitive and Developmental Systems, and an Associate Editor of the IEEE TRANSACTIONS ON COGNITIVE AND DEVELOPMENTAL SYSTEMS, the IEEE TRANSACTIONS ON NEURAL NETWORKS AND LEARNING SYSTEMS, and the *Journal of the Franklin Institute*, and has been on the editorial board of Entropy.

Pengju Ren (Member, IEEE) received the Ph.D. degree in electrical engineering from Xi'an Jiaotong University, Xi'an, China, in 2012.

From 2009 to 2011, he was a visiting Ph.D. student with the Computer Science and Artificial Intelligence Laboratory, Massachusetts Institute of Technology, Cambridge, MA, USA. He is currently an Associate Professor with the School of Electronic and Information Engineering, Xi'an Jiaotong University. His current research interests include novel computer architecture for machine learning and neuromorphic computing.

Authorized licensed use limited to: Bangladesh Univ of Engineering and Technology. Downloaded on April 14,2022 at 06:40:20 UTC from IEEE Xplore. Restrictions apply.

Nanning Zheng (Fellow, IEEE) received the graduation degree from the Department of Electrical Engineering, Xi'an Jiaotong University, Xi'an, China, in 1975, the M.S. degree in information and control engineering from Xi'an Jiaotong University, in 1981, and the Ph.D. degree in electrical engineering from Keio University, Yokohama, Japan, in 1985.

He joined Xi'an Jiaotong University in 1975, where he is currently a Professor and the Director of the Institute of Artificial Intelligence and Robotics. His research interests include computer vision, pattern recognition, and machine learning.

Prof. Zheng is the Chinese Representative on the Governing Board of the International Association for Pattern Recognition. He also serves as the President of the Chinese Association of Automation. He became a member of the Chinese Academy of Engineering in 1999.

Giacomo Indiveri (Senior Member, IEEE) received the M.Sc. degree in electrical engineering and the Ph.D. degree in computer science and electrical engineering from the University of Genova, Genova, Italy, in 1992 and 2004, respectively. He was a Post-Doctoral Research Fellow with the Division of Biology at Caltech and at the Institute of Neuroinformatics, University of Zurich and ETH Zurich. He was awarded an ERC Starting Grant on "Neuromorphic Processors" in 2011 and an ERC Consolidator Grant on neuromorphic cognitive agents in 2016. He is currently a Dual Professor at the Faculty of Science, University of Zurich, and the Department of Information Technology and Electrical Engineering, ETH Zurich, Switzerland. He is the Director of the Institute of Neuroinformatics (INI), University of Zurich and ETH Zurich. His research interests lie in the study of real and electronic neural processing systems, with a particular focus on spike-based learning and spike-based recurrent neural network dynamics. His research and development activities focus on the full custom hardware implementation of real-time sensory-motor systems using analog/digital neuromorphic circuits and emerging memory technologies.

Dr. Indiveri is a member of several technical committees of the IEEE Circuits and Systems Society and a fellow of the European Research Council.

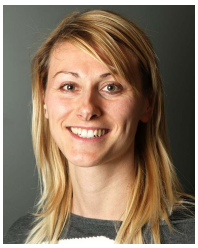

Elisa Donati (Member, IEEE) received the B.Sc. and M.Sc. degrees *(cum laude)* in biomedical engineering from the University of Pisa, Pisa, Italy, and the Ph.D. degree in BioRobotics from the Sant'Anna School of Advanced Studies, Pisa, Italy.

She is currently a Research Fellow at the Institute of Neuroinformatics, University of Zurich and ETHZ. Her research activities are at the interface of the neuroscience and the neuromorphic engineering. She is interested in understanding how the biological neural circuits carry out the computation and apply them in biomedical application and neurorobotics. She is investigating how to process EMG data to extract features to produce motor commands by using spiking neural networks. She was awarded a Marie Sklodowska-Curie Individual Fellowships on "Neuromorphic EMG Processing using Spiking Neural Networks" in 2017. She is the co-coordinator of the H2020 EU CSA project NEUROTECH.

Authorized licensed use limited to: Bangladesh Univ of Engineering and Technology. Downloaded on April 14,2022 at 06:40:20 UTC from IEEE Xplore. Restrictions apply.